Theory of the two-photon micromaser: Linewidth

A. H. Toor,* S.-Y. Zhu, and M. S. Zubairy*
Department of Physics, Hong Kong Baptist University, Kowloon Tong, Hong Kong
(Received 19 May 1995)

In this paper, we study the linewidth of a two-photon micromaser by using an exact Hamiltonian approach. We consider a three-level atomic system interacting with a single-mode radiation field. The intermediate level is considered to be off resonant with the field. In this model, under the large detuning limit, two-photon transitions result. We calculate the linewidth of a two-photon micromaser and present results in the small and large detuning limits. In the small detuning limit, single-photon behavior is evident, whereas in the large detuning limit, true two-photon behavior is exhibited. We compare the results for the linewidth, under a large detuning limit, with the results obtained by using a phenomenological, effective Hamiltonian approach. The absence of the dynamic Stark shift in a phenomenological, effective Hamiltonian leads to qualitatively different results in the two approaches.

PACS number(s): 84.40.Ik

I. INTRODUCTION

In a micromaser an atomic beam is injected in a high-Q microwave single-mode cavity. The atomic injection rate is kept low enough to ensure that there is just a single atom inside the cavity at one time. The experimental realization of a micromaser provides the simplest system for testing the predictions relating to atom-field interactions [1]. A number of effects have been predicted in a micromaser, which include trapping states and the generalization of nonclassical states [2] of the radiation field, e.g., number and squeezed states.

In addition to a large number of studies relating to the photon statistics of the radiation field inside a micromaser [3], a number of studies have also been done on the micromaser spectrum [4–7]. Some interesting features that are different from the usual Schawlow-Townes linewidth of the laser have been predicted. For example, it has been found that the linewidth of a micromaser can decrease with the increase of thermal photons [7].

In this paper, we are interested in the linewidth of a two-photon micromaser. It is well known that, in the two-photon processes, the high degree of correlation between the emitted photon pairs leads to some interesting nonclassical effects in quantum optics. The two-photon micromaser provides a clean setup for studying the two-photon processes. A two-photon micromaser was operated by Brune *et al.* [8] by using a niobium superconducting cavity with $Q \approx 10^8$, resonant at 68.415 87 GHz. They exploited the two-photon degenerate transition in rubidium atoms between the levels $40S_{1/2}$ and $39S_{1/2}$ through intermediate level $39P_{3/2}$ detuned from the cavity resonant mode.

A theory of two-photon micromaser was developed by Brune, Raimond, and Haroche [9] and Davidovich *et al.* [10]. Later Ashraf, Gea-Banacloche, and Zubairy [11] presented a theory of two-photon micromaser by using an exact Hamiltonian approach and obtained results for the photon statistics that were at variance with the results of Ref. [10]. They considered a three-level atomic system in a cascade configuration with the intermediate level arbitrarily detuned from the cavity field and derived the steady-state photon distribution function. They compared their results with the results obtained from the two-photon phenomenological, effective Hamiltonian approach, without dynamic Stark shift. Under the large detuning limit, they showed that the two approaches lead to the same results for the diagonal elements of the density operator. However, they pointed out that the approaches based on the exact Hamiltonian and the phenomenological effective Hamiltonian lead to different results for the off-diagonal elements of the density operator under this limit. A similar difference between the two approaches is shown in the two-photon atom-field interaction [12] and nondegenerate two-photon laser [13]. The exact Hamiltonian approach has also been used to study some other aspects of two-photon processes, for example, the two-photon correlated emission laser and [14] phase-sensitive amplification [15]. The two-photon dressed-state laser has been experimentally demonstrated [16] in recent past. The corresponding theory [17] for such a laser is based on the dressed-state picture, which includes the dynamic Stark shift.

In this paper, we extend the results of Ref. [11] to calculate the linewidth of a two-photon micromaser and study the effects of correlation among the emitted photon pairs. The micromaser linewidth is determined by the decay of the off-diagonal elements of the field density operator. We use an ansatz method that has been successfully used in the calculation of the linewidth of a laser and a single-photon micromaser to calculate the linewidth of a two-photon micromaser. We analyze our results in the limits of small and large detunings. In the small detuning limit, the two photons are uncorrelated and we obtain a behavior similar to that obtained in a single-photon micromaser. In the large detuning limit, a true two-photon behavior is exhibited. We compare the large detuning results with those obtained from a phenomenological, effective Hamiltonian approach and show that the two approaches lead to qualitatively different results.

*Permanent address: Department of Electronics, Quaid-i-Azam University, Islamabad 45320, Pakistan.

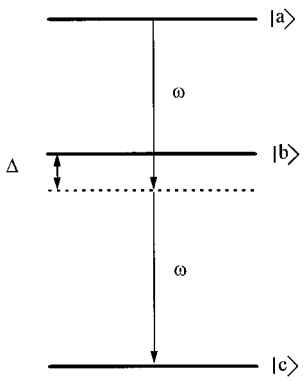

FIG. 1. Schematic diagram of the three-level atom interacting with a single-mode radiation field. The exact two-photon resonance is considered with arbitrary detuning Δ of the intermediate level $|b\rangle$.

II. EXACT HAMILTONIAN APPROACH

Consider an ensemble of three-level atoms, in a cascade configuration (see Fig. 1), interacting with the single mode of a radiation field inside a microwave cavity. The exact two-photon resonance is assumed such that the intermediate level $|b\rangle$ is detuned from the exact one-photon resonance, with the detuning given by (see Fig. 1)

$$\Delta=\omega-(\omega_a-\omega_b)=(\omega_b-\omega_c)-\omega, \tag{1}$$

where ω is the frequency of the resonant mode of the micromaser cavity. The frequencies associated with the atomic levels $|a\rangle$, $|b\rangle$, and $|c\rangle$ are ω_a, ω_b, and ω_c, respectively. The technological developments in the recent past have made it possible to achieve such an atomic configuration in the Rydberg states of alkali metals [8]. Our system, for $\Delta=0$, corresponds to two one-photon transitions $|a\rangle\rightarrow|b\rangle$ and $|b\rangle\rightarrow|c\rangle$. However, for sufficiently large values of Δ, the one-photon process is suppressed and the transition from $|a\rangle$ to $|c\rangle$ acquires a two-photon character.

The Hamiltonian in the interaction picture under the rotating-wave approximation for a system of a three-level atom in cascade configuration interacting with a single mode of a radiation field inside a cavity is

$$\begin{aligned}V_I=&\hbar g_1(a|a\rangle\langle b|e^{-i\Delta t}+a^\dagger|b\rangle\langle a|e^{i\Delta t})\\&+\hbar g_2(a|b\rangle\langle c|e^{i\Delta t}+a^\dagger|c\rangle\langle b|e^{-i\Delta t}),\end{aligned} \tag{2}$$

where g_1 and g_2 are the one-photon coupling constants corresponding to the atomic transitions $|a\rangle\rightarrow|b\rangle$ and $|b\rangle\rightarrow|c\rangle$, respectively. In a micromaser for a fixed length of the cavity, the velocity of the atoms determines the duration of the interaction time. Here we have assumed that the lifetimes of all three atomic levels involved are much larger than the interaction time. This justifies our ignoring the spontaneous decay to the other atomic levels, and the evolution of the atom-field combined density operator becomes unitary.

In accordance with the standard procedure used in laser theory, the difference between the field density operators after time τ, divided by the average time interval between the successive atoms, can be approximated by the differential equation [11]

$$\begin{aligned}\dot\rho_{n,m}(t)=&a_{n,m}\rho_{n,m}+b_{n-1,m-1}\rho_{n-1,m-1}+d_{n-2,m-2}\rho_{n-2,m-2}\\&+c_{n+1,m+1}\rho_{n+1,m+1},\end{aligned} \tag{3}$$

where

$$a_{n,m}=r_a(C_{a,n}C^*_{a,m}-1)-\frac{\gamma}{2}[2\overline{n_b}(n+m+1)+n+m], \tag{4}$$

$$b_{n,m}=r_aC_{b,n+1}C^*_{b,m+1}+\gamma\overline{n_b}\sqrt{(n+1)(m+1)}, \tag{5}$$

$$c_{n,m}=\gamma(\overline{n_b}+1)\sqrt{nm}, \tag{6}$$

$$d_{n,m}=r_aC_{c,n+2}C^*_{c,m+2}. \tag{7}$$

In writing Eq. (3) the cavity-loss terms are added in the usual way [18]. The cavity loss rate is denoted by γ and $\overline{n_b}$ is the average number of thermal photons in thermal equilibrium. The rate of injection of atoms is represented by r_a. The probability amplitudes $C_{a,n}$, $C_{b,n}$, and $C_{c,n}$ can be written, subject to the initial conditions that the atom and field are decoupled and the atoms are injected in the upper state $|a\rangle$, as

$$C_{a,n}=\frac{g_1^2(n+1)}{\beta_n\alpha_n^2}\,\eta_n(\tau)e^{-i(\Delta/2)\tau}+1, \tag{8}$$

$$C_{b,n+1}=-i\,\frac{g_1\sqrt{n+1}}{\beta_n}\,e^{i(\Delta/2)\tau}\sin\beta_n\tau, \tag{9}$$

$$C_{c,n+2}=\frac{g_1g_2\sqrt{(n+1)(n+2)}}{\beta_n\alpha_n^2}\,\eta_n(\tau)e^{-i(\Delta/2)\tau}. \tag{10}$$

In writing Eqs. (8)–(10) the following quantities have been introduced:

$$\eta_n(\tau)=\beta_n\cos\beta_n\tau+i\,\frac{\Delta}{2}\sin\beta_n\tau-\beta_ne^{i(\Delta/2)\tau}, \tag{11}$$

and

$$\alpha_n=\sqrt{g_1^2(n+1)+g_2^2(n+2)}, \tag{12}$$

$$\beta_n=\left(\frac{\Delta^2}{4}+\alpha_n^2\right)^{1/2}. \tag{13}$$

The photon statistics can be studied by setting $n=m$ in Eq. (3). In the steady state, the probability of finding n photons inside the cavity, i.e., the photon distribution function, $P(n)=\rho_{n,n}$, satisfies the following equation:

$$a_nP(n)+b_{n-1}P(n-1)+c_{n+1}P(n+1)+d_{n-2}P(n-2)=0, \tag{14}$$

where $a_n\equiv a_{n,n}$ and so forth. Moreover, it can be shown that

$$a_n+b_n+c_n+d_n=0. \tag{15}$$

Then the steady-state photon distribution function $P(n)$ can be written in terms of continued fractions

$$P(n)=P(0)\prod_{r=1}^{n}\frac{1}{c_r}\left[b_{r-1}+d_{r-1}+\frac{d_{r-2}c_{r-1}}{(b_{r-2}+d_{r-2})}+\cdots+\frac{d_0c_1}{b_0+d_1}\right], \tag{16}$$

where $P(0)$ is determined by the normalization condition. The photon statistics in a two-photon micromaser has been analyzed on the basis of this expression for the photon distribution function in Ref. [11]. In the next section we study the linewidth of a two-photon micromaser using an ansatz method attributable to Pedrotti, Scully, and Zubairy [19].

III. THE LINEWIDTH OF A TWO-PHOTON MICROMASER

The derivation of the linewidth requires a calculation of the two-time correlation function of the electric field, i.e., $\langle E^-(t)E^+(t+\tau)\rangle$. However, under the Markovian approximation, the quantum regression theorem implies that the time dependence of the two-time correlation function $\langle E^-(t)E^+(t+\tau)\rangle$ is identical to the time dependence of $\langle E^-(t)\rangle$. Hence the derivation of $\langle E^-(t)\rangle$ is sufficient to calculate the linewidth. Furthermore, this expectation value is related to the off-diagonal elements of the field density operation as

$$\langle E^-(t)\rangle\sim\langle a^\dagger(t)\rangle=\sum_{n=0}^{\infty}\sqrt{n+1}\,\rho_{n,n+1}(t). \tag{17}$$

Physically, this implies that the decay rate of the off-diagonal density operator $\rho_{n,n+1}(t)$ corresponds to the simultaneous decay of the field, which is responsible for the linewidth of the field. Our basic aim here is to determine the decay rate of $\rho_{n,n+1}(t)$.

The equation of motion for the elements of the field density operator, i.e., Eq. (3), can also be written in the form

$$\dot\rho_n^{(k)}=(a_n^{(k)}+b_n^{(k)}+c_n^{(k)}+d_n^{(k)})\rho_n^{(k)}+b_{n-1}^{(k)}\rho_{n-1}^{(k)}+c_{n+1}^{(k)}\rho_{n+1}^{(k)}+d_{n-2}^{(k)}\rho_{n-2}^{(k)}-(b_n^{(k)}+c_n^{(k)}+d_n^{(k)})\rho_n^{(k)}. \tag{18}$$

In writing Eq. (18) $\rho_n^{(k)}$ and $a_n^{(k)}$ stand for $\rho_{n,n+k}$ and $a_{n,n+k}$, respectively. At this point we suggest an ansatz for a steady-state solution for the off-diagonal elements of the field density operator, i.e., Eq. (18), in analogy with the corresponding solution of the diagonal elements of the field density operator [11], i.e.,

$$(b_n^{(k)}+c_n^{(k)}+d_n^{(k)})\rho_n^{(k)}=b_{n-1}^{(k)}\rho_{n-1}^{(k)}+d_{n-2}^{(k)}\rho_{n-2}^{(k)}+c_{n+1}^{(k)}\rho_{n+1}^{(k)}. \tag{19}$$

The solution of Eq. (18) is then of the form

$$\rho_n^{(k)}(t)=e^{-D_n^{(k)}(t)}\rho_n^{(k)}(0), \tag{20}$$

where $D_n^{(k)}(t)$ is some unknown function of n and t. On substituting this solution for $\rho_n^{(k)}(t)$ into Eq. (18) and using Eq. (19) we get

$$\dot D_n^{(k)}(t)=\frac{1}{2}\,\mu_n^{(k)}+(b_n^{(k)}+c_n^{(k)}+d_n^{(k)})(1-e^{-[D_{n-1}^{(k)}(t)-D_n^{(k)}(t)]})+c_{n+1}^{(k)}\frac{\rho_{n+1}^{(k)}(0)}{\rho_n^{(k)}(0)}(e^{-D_{n-1}^{(k)}(t)}-e^{-D_{n+1}^{(k)}(t)})e^{D_n^{(k)}}+d_{n-2}^{(k)}\frac{\rho_{n-2}^{(k)}(0)}{\rho_n^{(k)}(0)}(e^{-D_{n-1}^{(k)}(t)}-e^{-D_{n-2}^{(k)}(t)})e^{D_n^{(k)}}, \tag{21}$$

where

$$-\tfrac{1}{2}\mu_n^{(k)}=a_n^{(k)}+b_n^{(k)}+c_n^{(k)}+d_n^{(k)}. \tag{22}$$

So far our analysis is exact. Now we assume that $D_n^{(k)}(t)$ is a slowly varying function of n, which means that

$$|D_{n-1}^{(k)}(t)-D_n^{(k)}(t)|\ll 1, \tag{23}$$

and similarly $|D_{n-1}^{(k)}(t)-D_{n+1}^{(k)}(t)|$ and $|D_{n-1}^{(k)}-D_{n-2}^{(k)}|$ are much smaller than unity. Under this assumption Eq. (21) yields

$$D_n^{(k)}(t)\cong\tfrac{1}{2}\mu_n^{(k)}t. \tag{24}$$

It thus follows from Eq. (17) that

$$\langle a^\dagger(t)\rangle=\sum_{n=0}^{\infty}\sqrt{n+1}\;e^{-(1/2)\mu_n^{(1)}t}\rho_n^{(1)}(0). \tag{25}$$

Next we assume that $\mu_n^{(1)}$ is a slowly varying function of n. We can then replace $\mu_n^{(1)}$ in Eq. (25) by its mean value, i.e.,

$$\mu\equiv\langle\mu_n^{(1)}\rangle=\sum_{n=0}^{\infty}\mu_n^{(1)}P(n), \tag{26}$$

where the photon distribution function $P(n)$ is given by Eq. (16). Under this approximation, the micromaser spectrum is Lorentzian with the linewidth given by the real part of μ. An identical expression for linewidth can be obtained by using a factorization ansatz [20] or a London phase operator approach [7].

A. The limit of small detuning

In this limit our model corresponds to the two one-photon transitions, i.e., $|a\rangle\rightarrow|b\rangle$ and $|b\rangle\rightarrow|c\rangle$. The emission of the two photons is not correlated but still both transitions are influenced by the same cavity field.

In Fig. 2, the linewidth, i.e., the real part of μ, and the mean number of photons $\langle n\rangle$ are plotted versus the dimensionless interaction time $g\tau$ for $\overline{n_b}=0$. The sharp dips in the curve for the mean number of photons corresponds to the trapping states [21]

$$g\tau=\frac{2q\pi}{\sqrt{3}},\quad q=0,1,2,\ldots. \tag{27}$$

It has been shown in Ref. [11] that these trapping states correspond to the vacuum state, i.e., $|0\rangle$. However, for

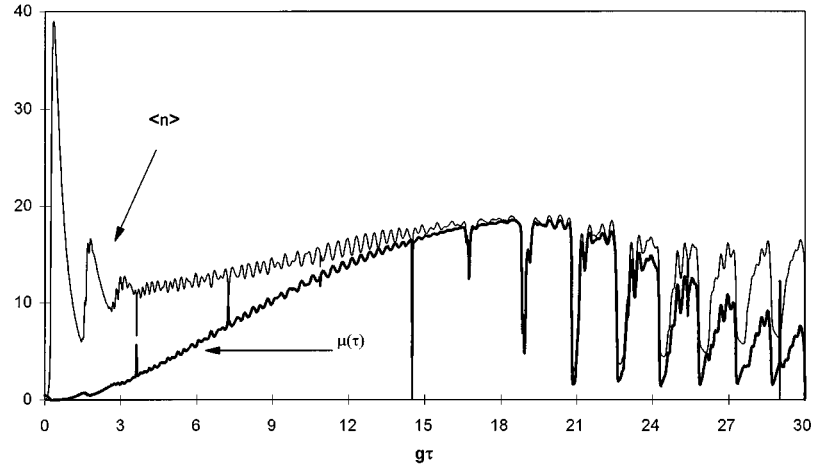

FIG. 2. Steady-state linewidth and average number of photons vs the dimensionless interaction time $g\tau$ for the cascade micromaser, i.e., $\Delta=0$, with $N_{\rm ex}\equiv r_a/\gamma=20$ at zero temperature, i.e., $\overline{n_b}=0$.

$\overline{n_b}\neq 0$ even the vacuum state does not qualify for the trapping state. In Fig. 3, the linewidth is plotted against the dimensionless interaction time for $\overline{n_b}=0$ and 5. A comparison of the linewidth for these two cases shows the reduction in linewidth due to thermal photons in a certain region. A similar reduction in the linewidth due to thermal photons is pointed out for the linewidth of the one-photon micromaser [7]. However, the effects of thermal photons on the laser linewidth are opposite. The smoothening of the dips corresponding to the trapping states for $\overline{n_b}=0$ can be seen due to the presence of the thermal photons.

B. The limit of large detuning

In the limit of large detuning of the intermediate level $|b\rangle$ with the cavity field mode, the probability of finding the atom in the level $|b\rangle$ is almost zero [11,12]. Under this condition our system corresponds to the true two-photon micromaser. The one-photon transitions become negligible (except for the one-photon transitions introduced to incorporate the effects of cavity loss) and the two-photon transitions become the most dominant one.

Let us introduce the two-photon effective coupling constant by taking $g_1=g_2\equiv g$, i.e.,

$$\lambda=\frac{g^2}{\Delta}, \tag{28}$$

and define

$$\epsilon=\frac{2\lambda}{\Delta}(2n+3). \tag{29}$$

Then, under the large detuning limit, i.e.,

$$8\frac{g^2 n}{\Delta^2}\ll 1, \tag{30}$$

β_n, given by Eq. (13), can be expanded as

$$\beta_n\approx\frac{\Delta}{2}+\frac{g^2}{\Delta}(2n+3). \tag{31}$$

The large detuning limit, i.e., Eq. (30), further implies that $\epsilon\ll 1$. The coefficients of the field density operator equation, i.e., Eqs (4)–(7), for $k=1$, reduce to the form

$$a_n^{(1)}=r_a\left[\frac{n+2}{2n+5}(e^{-i(2n+5)\lambda\tau}-1)+\frac{n+1}{2n+3}(e^{i(2n+3)\lambda\tau}-1)+\frac{(n+1)(n+2)}{(2n+3)(2n+5)}(e^{i(2n+3)\lambda\tau}-1)(e^{-i(2n+5)\lambda\tau}-1)\right]-\frac{r}{2}[4\overline{n_b}(n+1)+2n+1], \tag{32}$$

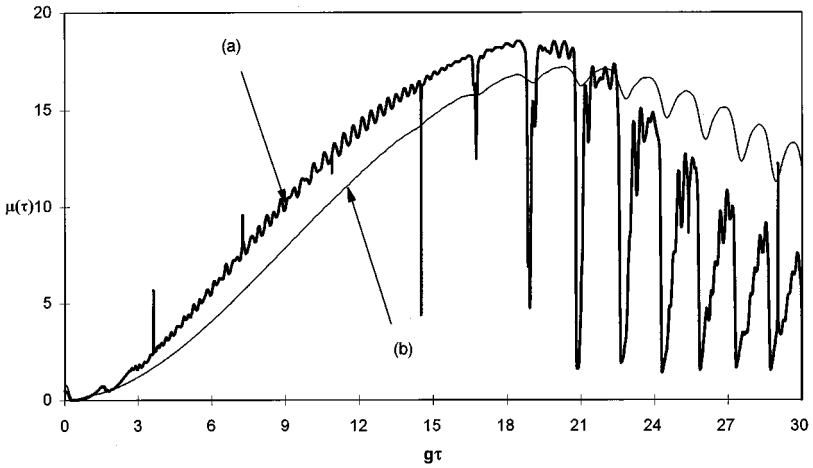

FIG. 3. Steady-state linewidth of the cascade micromaser, i.e., $\Delta=0$, vs the dimensionless interaction time $g\tau$ for (a) $\overline{n_b}=0$ and (b)$\overline{n_b}=5$. All other parameters are the same as in Fig. 2.

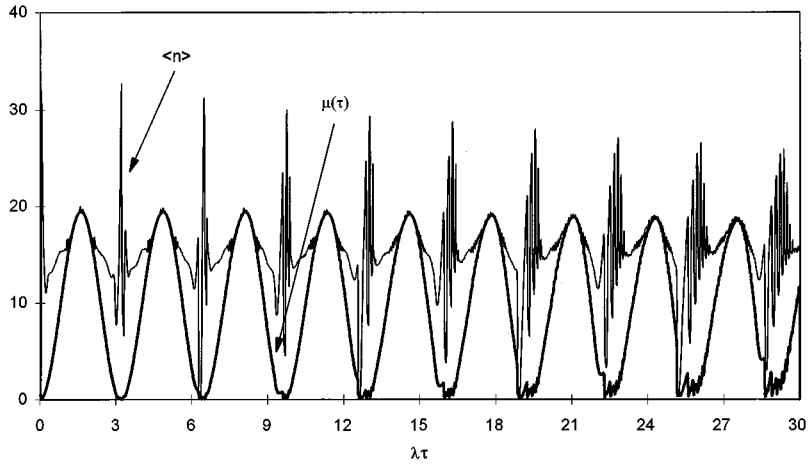

FIG. 4. Steady-state linewidth and average number of photons vs the dimensionless interaction time $\lambda\tau$ for the two-photon micromaser, i.e., $\Delta=50g$, with $N_{\rm ex}\equiv r_a/\gamma=20$ at zero temperature, i.e, $\overline{n_b}=0$.

$$b_n^{(1)}=\gamma\overline{n_b}\sqrt{(n+1)(n+2)}, \tag{33}$$

$$c_n^{(1)}=\gamma(\overline{n_b}+1)\sqrt{n(n+1)}, \tag{34}$$

$$d_n^{(1)}=r_a\left[\frac{(n+2)\sqrt{(n+1)(n+3)}}{(2n+3)(2n+5)}(e^{i(2n+3)\lambda\tau}-1)\times(e^{-i(2n+5)\lambda\tau}-1)\right]. \tag{35}$$

In writing Eqs. (32)–(35) we have ignored the terms of the order ϵ. The corresponding expression for the linewidth in the large detuning limit is

$$\mu(\tau)=-\mathrm{Re}\sum_{n=0}^{\infty}\left[r_a\left\{\frac{n+2}{2n+5}(e^{-i(2n+5)\lambda\tau}-1)+\frac{n+1}{2n+3}(e^{i(2n+3)\lambda\tau}-1)+\frac{(n+2)[(n+1)+\sqrt{(n+1)(n+3)}]}{(2n+3)(2n+5)}(e^{i(2n+3)\lambda\tau}-1)\times(e^{-i(2n+5)\lambda\tau}-1)\right\}-\gamma\overline{n_b}[2(n+1)-\sqrt{(n+1)(n+2)}-\sqrt{n(n-1)}]+\gamma[\sqrt{n(n+1)}-\tfrac{1}{2}(2n+1)]\right]\rho_{n,n}(\tau). \tag{36}$$

In Fig. 4, a comparison of the mean number of photons and the linewidth is made by plotting them against the dimensionless interaction time $\lambda\tau$ for $\Delta=50g$. It can be seen from the figure that the linewidth is a periodic function of the interaction time τ like the mean number of photons [11] but with a time period π/λ for the large values of n. The deviation from the perfect periodicity for the large values of the interaction time is due to the fact that the expansion of β_n, i.e., Eq. (31), does not hold for β_n as an argument of the trigonometric function under the large detuning limit, i.e., Eq. (30) [11,12]. The appropriate condition for the large detuning limit to justify the expansion of β_n as an argument of trigonometric function is

$$4n^2\left[\frac{g}{\Delta}\right]^2\lambda\tau\ll 1. \tag{37}$$

The presence of the thermal photons does not effect the linewidth at small dimensionless interaction times $\lambda\tau$. However, the significant effects of thermal photons on the line-

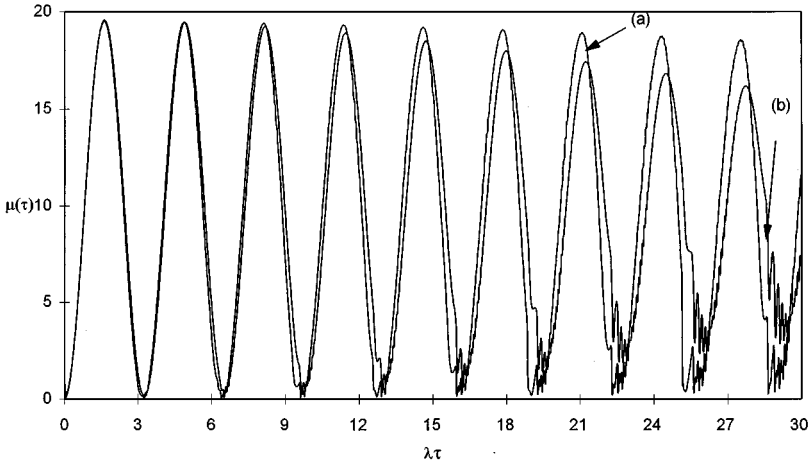

FIG. 5. Steady-state linewidth of the two-photon micromaser, i.e., $\Delta=50g$, vs the dimensionless interaction time $\lambda\tau$ for (a) $\overline{n_b}=0$ and (b) $\overline{n_b}=5$. All other parameters are the same as in Fig. 4.

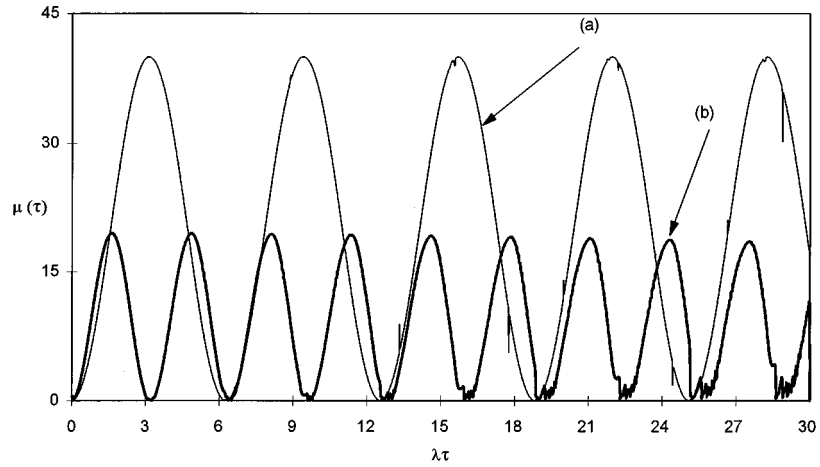

FIG. 6. Steady-state linewidth of the two-photon micromaser, i.e., $\Delta=50g$, for $N_{\rm ex}=20$ and $\overline{n}_b=0$ for (a) the phenomenological, effective Hamiltonian approach and (b) the exact Hamiltonian approach.

width of the two-photon micromaser for larger values of interaction time can be seen in Fig. 5.

IV. COMPARISON WITH THE PHENOMENOLOGICAL, EFFECTIVE HAMILTONIAN APPROACH

In the phenomenological effective Hamiltonian, the atomic levels $|a\rangle$ and $|c\rangle$ are coupled to the cavity field mode through a two-photon coupling constant. The Hamiltonian in the interaction picture under the rotating-wave approximation is

$$V_I=\hbar\lambda(|a\rangle\langle c|a^2+a^{\dagger 2}|c\rangle\langle a|), \tag{38}$$

where λ is the effective two-photon coupling constant.

The coefficients of the differential equation for the off-diagonal elements of the field density operator, i.e., Eq. (3), in the present case are modified as

$$a'_{n,m}=r_a(C'_{a,n}C'^{*}_{a,m}-1)-\frac{\gamma}{2}[2\overline{n}_b(n+m+1)+n+m], \tag{39}$$

$$b'_{n,m}=-\gamma\overline{n}_b\sqrt{(n+1)(m+1)}, \tag{40}$$

$$c'_{n,m}=\gamma(\overline{n}_b+1)\sqrt{nm}, \tag{41}$$

$$d'_{n,m}=r_aC'_{c,n+2}C'^{*}_{c,m+2}, \tag{42}$$

where the probability amplitudes $C'_{a,n}$ and $C'_{c,n+2}$ are given by [11,12]

$$C'_{a,n}=\cos\frac{\beta'_n}{2}\tau, \tag{43}$$

$$C'_{c,n+2}=-i\sin\frac{\beta'_n}{2}\tau, \tag{44}$$

with

$$\beta'_n=2\lambda\sqrt{(n+1)(n+2)}. \tag{45}$$

The expression for the linewidth in this approach becomes

$$\begin{aligned}\mu_{\rm eff}(\tau)=-{\rm Re}\sum_{n=0}^{\infty}\,(r_a\{&\cos[\sqrt{(n+1)(n+2)}\\&-\sqrt{(n+2)(n+3)}]\lambda\tau-1\}-\gamma\overline{n}_b[2(n+1)\\&-\sqrt{(n+1)(n+2)}-\sqrt{n(n+1)}]+\gamma[\sqrt{n(n+1)}\\&-\tfrac{1}{2}(2n+1)])\rho_{n,n}(\tau).\end{aligned} \tag{46}$$

We now compare the results of the linewidth obtained from the exact Hamiltonian approach under large detuning limit with that obtained from the phenomenological effective Hamiltonian approach. In Fig. 6, the linewidth for the exact Hamiltonian (under large detuning limit) and phenomenological effective Hamiltonian approach are plotted for $\overline{n}_b=0$ and $N_{\rm ex}\equiv r_a/\gamma=20$. The obvious difference can be explained by looking at the two expressions, i.e., Eqs. (36) and (46), for $n\gg1$. The expression for the linewidth in the phenomenological effective Hamiltonian approach for $n\gg1$, which means $\beta'_n\approx\lambda(2n+3)$, can be written in the form

$$\begin{aligned}\mu_{\rm eff}(\tau)=-{\rm Re}\sum_{n=0}^{\infty}\,&\{r_a[\tfrac{1}{2}(e^{-2i\lambda\tau}+1)e^{i\lambda\tau}-1]\\&-\gamma\overline{n}_b[2(n+1)-\sqrt{(n+1)(n+2)}-\sqrt{n(n+1)}]\\&+\gamma[\sqrt{n(n+1)}-\tfrac{1}{2}(2n+1)]\}\rho_{n,n}(\tau).\end{aligned} \tag{47}$$

Similarly, the expression for the linewidth in the exact Hamiltonian approach under large detuning limit reduces to the following form for $n\gg1$:

$$\begin{aligned}\mu(\tau)=-{\rm Re}\sum_{n=0}^{\infty}\,&\{r_a[\tfrac{1}{2}(e^{-2i\lambda\tau}+1)-1]-\gamma\overline{n}_b[2(n+1)\\&-\sqrt{(n+1)(n+2)}-\sqrt{n(n+1)}]+\gamma[\sqrt{n(n+1)}\\&-\tfrac{1}{2}(2n+1)]\}\rho_{n,n}(\tau).\end{aligned} \tag{48}$$

Expressions (47) and (48) for the linewidth are identical apart from an additional phase factor, i.e., $e^{i\lambda\tau}$ with the term proportional to r_a in the results for phenomenological effective Hamiltonian approach. It can be seen from the above equations that the linewidth in both approaches is a periodic

function of τ but with different periods. In the phenomenological effective Hamiltonian approach, the period is $2\pi/\lambda$ with a maximum value approximately equal to $2N_{ex}$. On the other hand, in the exact Hamiltonian approach, the period is π/λ with the maximum value approximately equal to N_{ex}. This difference is due to the additional phase factor, which is the result of the neglect of Stark shift in the phenomenological effective Hamiltonian approach.

[1] D. Meschede, H. Walther, and G. Müller, Phys. Rev. Lett. **54**, 551 (1985); S. Haroche and J. M. Raimond, Adv. At. Mol. Opt. Phys. **20**, 414 (1985); G. Rempe, H. Walther, and N. Klein, Phys. Rev. Lett. **58**, 508 (1987).

[2] P. Filipowicz, J. Javanainen, and P. Meystre, J. Opt. Soc. Am. B **3**, 906 (1986); J. Krause, M. O. Scully, and H. Walther, Phys. Rev. A **36**, 4547 (1987); J. Krause, M. O. Scully, T. Walther, and H. Walther, *ibid.* **39**, 1915 (1989); J. J. Slosser, P. Meystre, and S. L. Braunstein, Phys. Rev. Lett. **63**, 934 (1989); S. Qamar, K. Zaheer, and M. S. Zubairy, Opt. Commun. **78**, 341 (1990).

[3] G. Rempe and H. Walther, Phys. Rev. A **42**, 1650 (1990); H. Paul and Th. Richter, Opt. Commun. **85**, 508 (1991); H.-J. Briegel, B.-G. Englert, N. Sterpi, and H. Walther, Phys. Rev. A **49**, 2962 (1994); C. Wagner, A. Schenzle, and H. Walther, Opt. Commun. **107**, 318 (1994).

[4] S. Qamar and M. S. Zubairy, Phys. Rev. A **44**, 7804 (1991).

[5] M. O. Scully, H. Walther, G. S. Agarwal, T. Quang, and W. Schleich, Phys. Rev. A **44**, 5992 (1991).

[6] N. Lu, Phys. Rev. Lett. **70**, 912 (1993); Phys. Rev. A **47**, 1347 (1993).

[7] T. Quang, G. S. Agarwal, J. Bergau, M. O. Scully, H. Walther, K. Vogel, and W. Schleich, Phys. Rev. A **48**, 803 (1993); K. Vogel, P. Schleich, M. O. Scully, and H. Walther, *ibid.* **48**, 813 (1993).

[8] M. Brune, J. M. Raimond, P. Goy, L. Davidovich, and S. Haroche, Phys. Rev. Lett. **59**, 1899 (1987).

[9] M. Brune, J. M. Raimond, and S. Haroche, Phys. Rev. A **35**, 154 (1987).

[10] L. Davidovich, J. M. Raimond, M. Brune, and S. Haroche, Phys. Rev. A **36**, 3771 (1987).

[11] I. Ashraf, J. Gea-Banacloche, and M. S. Zubairy, Phys. Rev. A **42**, 6704 (1990); see also, I. Ashraf and M. S. Zubairy, Opt. Commun. **77**, 85 (1990).

[12] A. H. Toor and M. S. Zubairy, Phys. Rev. A **45**, 4951 (1992).

[13] A. W. Boone and S. Swain, Quantum Opt. **1**, 27 (1989); Opt. Commun. **73**, 47 (1989).

[14] M. O. Scully, Phys. Rev. Lett. **55**, 2802 (1985); M. O. Scully and M. S. Zubairy, Phys. Rev. A **35**, 752 (1987); J. Bergou, M. Orszag, and M. O. Scully, *ibid.* **38**, 754 (1988); M. O. Scully, K. Wodkiewicz, M. S. Zubairy, J. Bergou, N. Lu, and J. Meyer-ter-Vehn, Phys. Rev. Lett. **60**, 1832 (1988).

[15] M. O. Scully and M. S. Zubairy, Opt. Commun. **66**, 303 (1988); N. A. Ansari, J. Gea-Banacloche, and M. S. Zubairy, Phys. Rev. A **41**, 5179 (1990).

[16] Y. Zhu, A. Lezama, and T. W. Mossberg, Phys. Rev. A **39**, 2268 (1989); A. Lezama, Y. Zhu, M. Kanskar, and T. W. Mossberg, *ibid.* **41**, 1570 (1990); G. Khitrova, J. F. Valley, and H. M. Gibbs, Phys. Rev. Lett. **60**, 1126 (1988).

[17] M. Lewenstien, Y. Zhu, and T. W. Mossberg, Phys. Rev. Lett. **64**, 3131 (1990); J. Zakrzewski, M. Lewenstien, and T. W. Mossberg, Phys. Rev. A **44**, 7717 (1991); **44**, 7732 (1991); **44**, 7746 (1991).

[18] See, for example, M. Sargent III, M. O. Scully, and W. E. Lamb, Jr., *Laser Physics* (Addison-Wesley, Reading, MA, 1974), Chap. 17.

[19] L. Pedrotti, M. O. Scully, and M. S. Zubairy, in *Coherence and Quantum Optics VI*, edited by L. Mandel and E. Wolf (Plenum, New York, 1984), p. 899.

[20] M. O. Scully and W. E. Lamb, Jr., Phys. Rev. **159**, 208 (1967).

[21] P. Meystre, G. Rempe, and H. Walther, Opt. Lett. **13**, 1078 (1988).